Technologies for Analyzing the Optic Disc, RNFL, and Macula

Optical Coherence Tomography

By Lindsey S. Folio, BSc; Gadi Wollstein, MD; and Joel S. Schuman, MD

Glaucoma can be characterized as a slowly progressing optic neuropathy that damages the retinal ganglion cells (RGCs) and their axons. This damage causes thinning of the retinal nerve fiber layer (RNFL), leads to cupping of the optic nerve head (ONH), and usually results in observable visual field loss. Because glaucomatous damage is irreversible, early detection is crucial for effective treatment through medical or surgical methods to halt further progression and preserve functional vision. Studies have shown that up to half of the RGCs could be damaged before defects are reported on the visual field.[1] A more resolute, objective method of identifying glaucoma is therefore needed for at-risk patients.

Ophthalmic imaging techniques such as optical coherence tomography (OCT) allow objective, quantitative evaluation of ocular structures. OCT has been shown to

TABLE 1. COMMERCIALLY AVAILABLE SD-OCT DEVICES

Device	Company	Axial Resolution	Scanning Speed (A-scans/sec)	Summary
Bioptigen SD-OCT	Bioptigen (Research Triangle Park, NC)	4 µm	20,000	Designed for clinical and research use. Offers a handheld probe, microscope attachment, and freedom to change scanning protocols to meet user's needs.
Cirrus HD-OCT	Carl Zeiss Meditec, Inc. (Dublin, CA)	5 µm	27,000	The software includes guided progression analysis for detection of glaucomatous progression.
Spectralis OCT	Heidelberg Engineering GmbH (Heidelberg, Germany)	4 µm	40,000	A high-speed SD-OCT device that includes eye tracking, fluorescein angiography, indocyanine green angiography, and autofluorescence.
Spectral OCT SLO	Opko Health, Inc. (Miami, FL)	6 µm	27,000	Combines SD-OCT, scanning laser ophthalmoscopy, and microperimetry in one device.
RTVue-100	Optovue Inc. (Fremont, CA)	5 µm	26,000	Offers multiple scanning protocols for glaucoma, including retinal nerve fiber layer, optic nerve head, and ganglion cell complex analysis.
SOCT Copernicus	Optopol (Zawiercie, Poland)	5 µm	27,000	Contains progression analysis software that uses the disk damage likelihood scale, asymmetry between the discs, and retinal nerve fiber layer thickness to determine progression.
3D-OCT 2000	Topcon Medical Systems, Inc. (Oakland, NJ)	5 µm	27,000	Combines SD-OCT with a high-resolution fundus camera.

correlate well with histological retinal measurements[2] and to allow direct visualization and quantification of the structures of the retina and ONH. This device is a valuable tool for detecting glaucoma[3-5] and monitoring its progression.[6]

CONCEPTS

Time Domain OCT

OCT was first described by Huang et al in 1991 as a high-resolution, cross-sectional imaging technique that functions similarly to ultrasound but uses light instead of sound.[7] The imaging process involves low-coherence near-infrared light, which is split and directed at a moving reference mirror and the tissue of interest. The two light beams are then reflected and recombine at an interferometer, where an interference pattern is produced and assessed by a photodetector. This procedure is repeated along a line to form a cross-section of the tissue imaged. Time domain OCT (TD-OCT) has an axial resolution of approximately 10 µm and can scan at an average rate of 400 axial scans/sec.

Spectral Domain OCT

Spectral domain OCT (SD-OCT) for ophthalmic imaging was first described by Wojtkowski et al in 2002.[8] Unlike TD-OCT, SD-OCT does not require the mirror in the reference arm to move, because all information is encoded simultaneously in the frequency spectrum. SD-OCT allows scanning speeds of up to 55,000 axial scans/sec with axial resolutions of 5 to 6 µm.[9] The faster scanning speed permits the acquisition of three-dimensional datasets, which allows extensive postprocessing of the data without requiring the patient to remain in front of the device. The increased resolution has resulted in improved visualization of retinal layers. Some studies have shown SD-OCT imaging to have a greater diagnostic ability for glaucoma compared with TD-OCT,[10,11] whereas others have shown equivalence.[12,13] Table 1 shows currently commercially available SD-OCT devices.

IMAGING STRUCTURES FOR GLAUCOMA

Optic Disc

The common scanning patterns used to assess the optic disc in glaucoma include a high-density raster scan (cube) or a radial scan. Figure 1 was obtained with an Optic Disc Cube 200 X 200 scan (Cirrus HD-OCT; Carl Zeiss Meditec, Inc., Dublin, CA) of a patient with glaucoma that covered a 6- X 6-mm area centered on the ONH. The OCT image is analyzed using automated detection of the disc's boundaries. Cup-to-disc ratios, disc and rim area, and cup-volume measurements are calculated from the data and displayed. Images can be corrected for ocular movement during scanning by aligning the OCT data using the en face image (Figure 1A). The en face image represents an aerial view of the scanned area and can be used to detect ocular movement during image acquisition that might affect the reliability of the reported measurements. Eye movements will cause discontinuities in blood vessels and an anomalous appearance to the disc. Studies have shown that analysis of the ONH with SD-OCT can differentiate between healthy and glaucomatous eyes.[14]

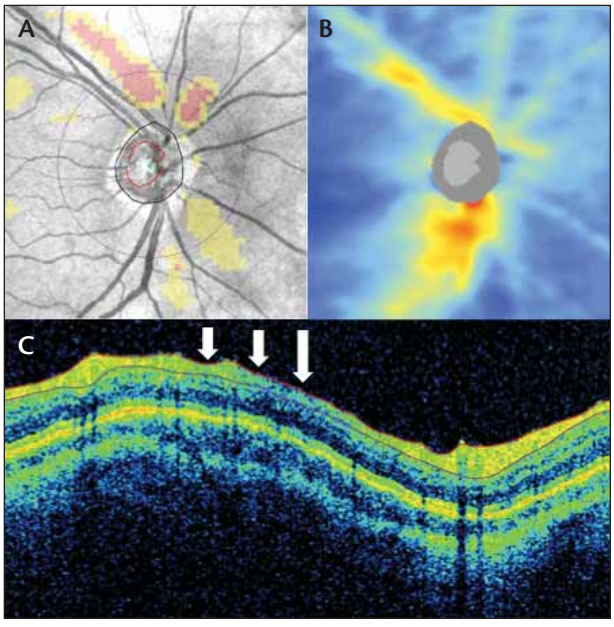

Figure 1. SD-OCT obtained an optic disc cube 200 X 200 scan of the right eye of a patient with glaucoma. The en face image shows the boundaries of the cup (red) and disc (black) as well as the deviation of the RNFL thickness from a normative distribution (yellow and red clusters) in the superotemporal and inferonasal regions (A). On the RNFL thickness map, thinning is evident in the superior pole (B). In the circumpapillary cross-section image sampled from the 3.4-mm-diameter circle on cube scan, white arrows indicate focal thinning (C).

RNFL

Peripapillary thinning of the RNFL is a hallmark of glaucoma and represents axonal loss due to the RGC damage. In OCT imaging, the RNFL appears as a highly reflective layer at the vitreoretinal interface that is automatically segmented by the software. An RNFL thickness map (Figure 1B) is generated from the scanned cube, allowing visualization of potential RNFL thinning within the cube. Circumpapillary analysis can be performed by sampling from the cube of data along a 3.4-mm-diameter circular scan centered on the ONH (Figure 1A and C). Alternatively, RNFL thickness can be obtained by

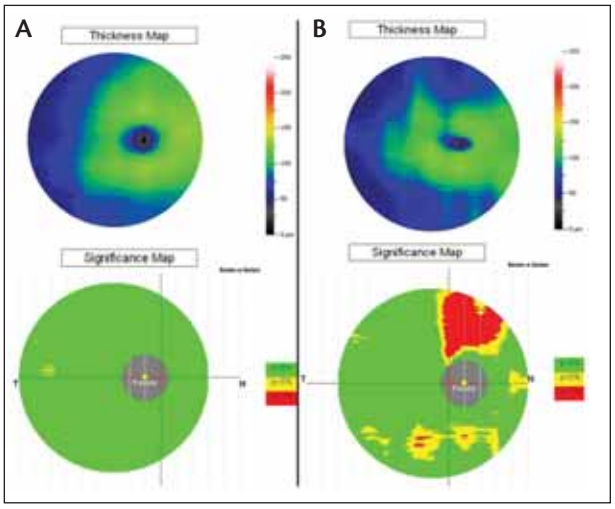

Figure 2. SD-OCT GCC thickness and significant deviation from normal maps. A healthy patient has a normal GCC thickness and no deviation from normal in the significance map (A). The same patient shown in Figure 1 has superior GCC abnormalities indicated by reduced thickness and significant thinning (B). Images obtained with the RTVue-100 (Optovue Inc., Fremont, CA).

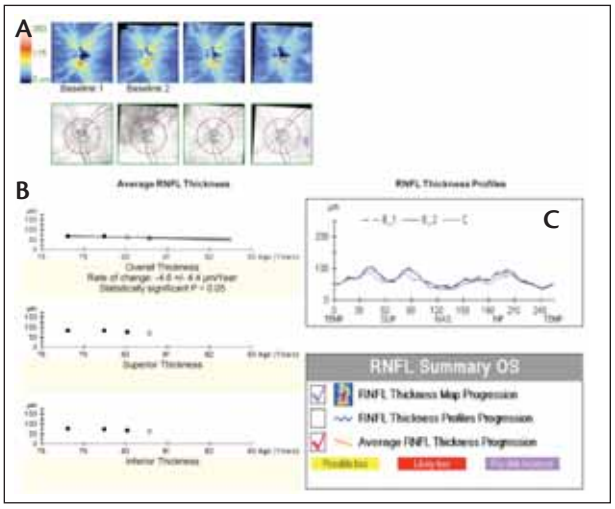

Figure 3. SD-OCT glaucoma progression analysis for four visits over a 2-year follow-up. The RNFL thickness maps show a global thinning, as evidenced by the disappearing red and yellow coloring along the retinal nerve fiber bundle paths (A). The average RNFL thickness on the 3.4-mm-diameter circle indicates likely progression over the follow-up period (B). The RNFL thickness profiles show a decreased thickness, but it is not designated as possible or likely progression by the SD-OCT software (C). Images obtained with Cirrus HD-OCT.

performing a 3.4-mm-diameter circular scan (rather than a cube), but sampling from a cube scan allows the location of the circle to be repositioned and matched between visits.

RNFL thickness is presented with a comparison to a normative distribution of age-matched healthy subjects. Typically, the RNFL thickness profile demonstrates an increased thickness in the superior and inferior positions, giving a double-hump pattern. OCT image analysis software also reports the average RNFL thickness as well as quadrant and clock-hour thicknesses in the 3.4-mm circle. Measured quadrant and clock-hour thicknesses can also be compared to a normative distribution of age-matched healthy subjects and are important in testing for local glaucomatous defects. OCT has been shown to produce accurate and reproducible RNFL thickness measurements.[15] Additionally, some studies have shown SD-OCT analysis of the RNFL to be a better diagnostic tool for glaucoma than analysis of the ONH.[16]

Macula

Glaucoma damages the RGCs, and approximately 50% of these cells are located in the macular region.[17] They have been observed to compose 30% to 35% of the retinal thickness in the macula, making the macular inner layers a potential target for glaucoma detection.[18] Several scanning patterns are commonly used to image the macula, including a high-density raster scan (cube), spoke pattern radial scans centered on the fovea, and a mesh scan pattern (combination of vertical and horizontal scans). With the improved resolution and higher sampling rate of SD-OCT, automated quantification of the inner retinal layers is possible, thus specifically targeting the layers prone to glaucomatous damage. The ganglion cell complex (GCC) analysis (Figure 2) has been shown to provide a better glaucoma diagnostic parameter than total retinal thickness of the macula.[19]

MONITORING GLAUCOMATOUS PROGRESSION WITH OCT

Glaucomatous progression can be identified in the form of narrowing of the neuroretinal rim and thinning of the RNFL and/or GCC. The proven reproducibility of RNFL measurements obtained with OCT designate these values as potential parameters to measure structural changes over time.[15] Both TD-OCT and SD-OCT use software that assesses progression by plotting a linear regression of RNFL thickness against age (Figure 3). Progression studies have found TD-OCT progression analysis capable of identifying local and diffuse loss of RNFL, and they have shown the rate of RNFL thinning to exceed the rate of progression determined by visual field testing.[6,20]

Because SD-OCT is a relatively recent technology, more longitudinal data need to be collected before studies can test its ability to detect disease progression. We predict SD-OCT will surpass TD-OCT's ability because of the higher sampling densities, improved scanning density, better reproducibility,[21] and its image-registration capabilities.

Lindsey S. Folio, BSc, is a research specialist for the Department of Ophthalmology at the University of Pittsburgh School of Medicine and a graduate student in the Department of Bioengineering, Swanson School of Engineering at the University of Pittsburgh. She acknowledged no financial interest in the products or companies mentioned herein.

Gadi Wollstein, MD, is an associate professor of ophthalmology at the University of Pittsburgh School of Medicine and the director of the Ophthalmic Imaging Research Laboratories at the UPMC Eye Center. He has received research funds from Carl Zeiss Meditec, Inc., and Optovue Inc. Dr. Wollstein may be reached at wollsteing@upmc.edu.

Joel S. Schuman, MD, is the Eye and Ear Foundation professor and chairman of the Department of Ophthalmology at the University of Pittsburgh School of Medicine, and he is the director of the UPMC Eye Center. He is also a professor of bioengineering at the University of Pittsburgh School of Engineering and a professor at the Center for the Neural Basis of Cognition, Carnegie Mellon University and University of Pittsburgh. Dr. Schuman has received lecture fees and payment of faculty travel expenses from Pfizer, Inc. He receives royalties from intellectual property licensed by M.I.T. to Carl Zeiss Meditec, Inc.

1. Quigley HA, Dunkelberger GR, Green WR. Retinal ganglion cell atrophy correlated with automated perimetry in human eyes with glaucoma. *Am J Ophthalmol.* 1989;107(5):453-464.
2. Gloesmann M, Hermann B, Schubert C, et al. Histologic correlation of pig retina radial stratification with ultrahigh-resolution optical coherence tomography. *Invest Ophthalmol Vis Sci.* 2003;44(4):1696-703.
3. Schuman JS, Hee MR, Puliafito CA, et al. Quantification of nerve fiber layer thickness in normal and glaucomatous eyes using optical coherence tomography. *Arch Ophthalmol.* 1995;113(5):586-596.
4. Hee MR, Izatt JA, Swanson EA, et al. Optical coherence tomography of the human retina. *Arch Ophthalmol.* 1995;113(3):325-332.
5. Badala F, Nouri-Mahdavi K, Raoof DA, et al. Optic disc and nerve fiber layer imaging to detect glaucoma. *Am J Ophthalmol.* 2007;144(5):724-732.
6. Wollstein G, Schuman JS, Price LL, et al. Optical coherence tomography longitudinal evaluation of retinal nerve fiber layer thickness in glaucoma. *Arch Ophthalmol.* 2005;123(4):464-470.
7. Huang D, Swanson EA, Lin CP, et al. Optical coherence tomography. *Science.* 1991;254(5035):1178-1181.
8. Wojtkowski M, Leitgeb R, Kowalczyk A, et al. In vivo human retinal imaging by Fourier domain optical coherence tomography. *J Biomed Opt.* 2002;7(3):457-463.
9. Wojtkowski M, Srinivasan V, Ko T, et al. Ultrahigh-resolution, high-speed, Fourier domain optical coherence tomography and methods for dispersion compensation. *Opt Express.* 2004;12(11):2404-2422.
10. Sung KR, Kim DY, Park SB, et al. Comparison of retinal nerve fiber layer thickness measured by Cirrus HD and Stratus optical coherence tomography. *Ophthalmology.* 2009;116(7):1264-1270.
11. Vizzeri G, Balasubramanian M, Bowd C, et al. Spectral domain-optical coherence tomography to detect localized retinal nerve fiber layer defects in glaucomatous eyes. *Opt Express.* 2009;17(5):4004-4018.
12. Sehi M, Grewal DS, Sheets CW, et al. Diagnostic ability of Fourier-domain vs time-domain optical coherence tomography for glaucoma detection. *Am J Ophthalmol.* 2009;148(4):597-605.
13. Jeoung JW, Park KH. Comparison of Cirrus OCT and Stratus OCT on the ability to detect localized retinal nerve fiber layer defects in preperimetric glaucoma. *Invest Ophthalmol Vis Sci.* 2010;51(2):938-945.
14. Li S, Wang X, Wu G, et al. Evaluation of optic nerve head and retinal nerve fiber layer in early and advance glaucoma using frequency-domain optical coherence tomography. *Graefes Arch Clin Exp Ophthalmol.* 2009;248(3):429-434.
15. Schuman JS, Pedut-Kloizman T, Hertzmark E, et al. Reproducibility of nerve fiber layer thickness measurements using optical coherence tomography. *Ophthalmology.* 1996;103(11):1889-1898.
16. Rao HL, Zangwill LM, Weinreb RN, et al. Comparison of different spectral domain optical coherence tomography scanning areas for glaucoma diagnosis. Ophthalmology. In press.
17. Curcio CA, Allen KA. Topography of ganglion cells in human retina. *J Comp Neurol.* 1990;300(1):5-25.
18. Zeimer R, Asrani S, Zou S, et al. Quantitative detection of glaucomatous damage at the posterior pole by retinal thickness mapping. A pilot study. *Ophthalmology.* 1998;105(2):224-231.
19. Mori S, Hangai M, Sakamoto A, et al. Spectral-domain optical coherence tomography measurement of macular volume for diagnosing glaucoma. *J Glaucoma.* In press.
20. Leung CK, Cheung CY, Weinreb RN, et al. Evaluation of retinal nerve fiber layer progression in glaucoma: a study on optical coherence tomography guided progression analysis. *Invest Ophthalmol Vis Sci.* 2009;51(1):217-222.
21. Kim JS, Ishikawa H, Sung KR, et al. Retinal nerve fibre layer thickness measurement reproducibility improved with spectral domain optical coherence tomography. *Br J Ophthalmol.* 2009;93(8):1057-1063.

Scanning Laser Polarimetry

By Neil T. Choplin, MD

Scanning laser polarimetry (SLP) uses a physical property inherent to the retinal nerve fiber layer (RNFL) to assess its thickness in vivo with a high degree of sensitivity and specificity for diagnosing glaucoma.

PRINCIPLES

Of the three computerized scanning imaging techniques currently available to evaluate the RNFL, SLP is the only one that uses a physical property of the RNFL other than reflectivity to make its assessments. This property, called *form birefringence,* arises in a material or tissue composed of substructures smaller in diameter than the wavelength of light used to image it. A polarized light passing through such a tissue will undergo a measurable phase shift, called *retardation,* which is directly proportional to the thickness of the tissue. Microtubules contained within the individual fibers of the RNFL give rise to its birefringent properties.[1]

The commercially available scanning laser polarimeter, the GDx VCC (Carl Zeiss Meditec, Inc., Dublin, CA) assesses the RNFL by passing a polarized light through it and measuring the resultant retardation by an ellipsometer. Although retardation is measured in angular degrees, it is proportional to thickness and is expressed in microns.

This is based on the relationship between the amount of retardation and the histologically determined RNFL thickness found in monkey eyes.[2] Birefringence inherent to structures in the anterior segment, mostly the cornea, is subtracted by a compensator that is individually adjusted for the eye being assessed (variable corneal compensation [VCC]).[3] The latest version of the instrument incorporates a software correction for eyes with low signal-to-noise ratios called *enhanced corneal compensation* or ECC. Using individualized anterior segment compensation allows the results of SLP to better match the appearance of the RNFL by red-free fundus photography.[4]

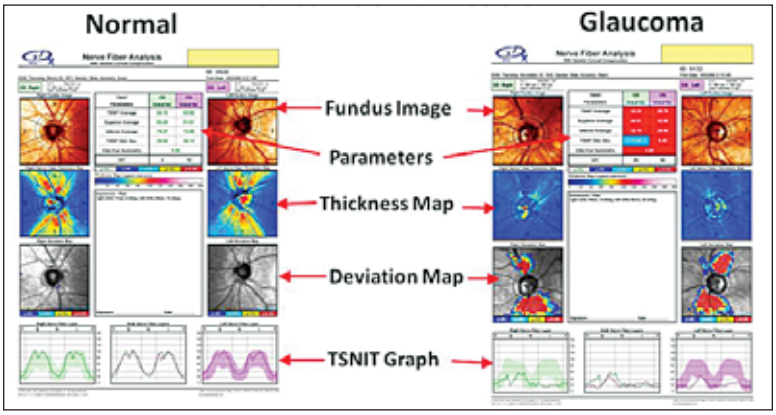

Figure 1. Printout from the GDx VCC.

CLINICAL MEASUREMENTS

After patient-identifying information, including birth date and race, are entered, SLP assesses anterior segment birefringence with the method described by Zhou and Weinreb.[3] The software automatically adjusts the anterior segment compensator. RNFL thickness can then be assessed with eye-specific corneal compensation in a 20° X 20° field of view at a resolution of 128 pixels X 128 pixels. Usually, the right eye is measured first, followed by the left eye.

The GDx software positions a circle, 8 pixels wide with an inner diameter of 54 pixels, so that it is centered on the optic nerve image. This circle is known as the *TSNIT plot*, because it contains RNFL values going from the temporal side of the optic nerve, then superiorly, nasally, inferiorly, and back to temporally. Based on the retardation values within this band, the software calculates six parameters: TSNIT average, superior average, inferior average, TSNIT standard deviation, inter-eye symmetry, and nerve fiber indicator (NFI). The NFI is the value derived from a support vector-machine–derived algorithm trained to discriminate between healthy and glaucomatous eyes. Possible values range from 1 (normal) to 100 (glaucoma) on a linear scale.

Results are displayed for both eyes on a single page (Figure 1). The printout features a reflectance image that is used for orientation and assessment of image quality. The retardation image (thickness map) presents the measurements of retardation in a 20° X 20° area around the optic nerve head, color coded for value. Bright, warm colors represent thicker areas, and dark, cool colors represent thinner areas. Parameters and the TSNIT plot are constructed from measurements within the measurement circle. The deviation map shows how the measurements compare to an age- and race-matched normative database. Points that are outside normal limits are flagged according to statistical significance. This map is comparable to the Humphrey Field Analyzer's (Carl Zeiss Meditic, Inc.) total deviation probability plot. The TSNIT plot (temporal-superior-nasal-inferior-temporal) displays retardation in the measurement circle (dark line). The normal 95% range is shown as a shaded area; the yellow area represents values between the first and fifth percentiles, whereas values in the red area are below the first percentile. The parameters that are within normal limits (above the fifth percentile) are shown in green on the printout. Parameters that are outside normal limits are shown in white on a shaded background, with the shading corresponding to its percentile in the normative database (yellow between the first and fifth percentile, red below the first percentile).

DIAGNOSTIC ACCURACY

The NFI is the one parameter of the GDx VCC showing the greatest ability to discriminate between glaucomatous and normal eyes.[5] In a group of 73 healthy subjects and 146 glaucoma patients of similar age, the sensitivity and specificity of the NFI were 89% and 96%, respectively, at a cutoff value of 40 (GDx VCC software version 5.0.1). At the same specificity of 96%, the sensitivity to detect mild, moderate, and severe glaucoma—classified by the severity of the patients' visual field mean deviation score—was 84%, 87%, and 100%, respectively. The relatively low sensitivity for early glaucoma may be due to the fact that the parameters are relatively insensitive to focal defects; these would easily be seen on the deviation map. With the latest software versions of the GDx VCC (version 5.3.1 and later), similar results are seen with the cutoff level at 35.

INTERPRETATION OF PRINTOUTS

When interpreting GDx VCC measurements, clinicians should expect some variability in the appearance of the

RNFL. In addition, they should keep in mind that one out of every 20 healthy subjects might be expected to have parameters that are flagged at $P < 5\%$. In the retardation maps of healthy eyes, retardation is always present adjacent to the thicker blood vessels superior and inferior to the optic disc. The appearance of the RNFL may vary significantly between subjects. The deviation map usually shows no flagged pixels. Flagged (false positive) areas may occur in the nasal half of the map in healthy subjects. The TSNIT plot shows a "double-hump" pattern (corresponding to a thicker RNFL superiorly and inferiorly), although the appearance of the TSNIT plot may vary considerably between subjects. The plot is usually within the green area. In healthy eyes, the TSNIT plots of both eyes are symmetrical. Asymmetry may occur in the nasal areas. In healthy eyes, the NFI is usually below 35.

In glaucomatous eyes, defects of the RNFL often develop superotemporal and inferotemporal to the optic disc. Loss may be localized, is sometimes visible as a clear wedge-shaped defect, and may be diffuse. In the retardation maps of glaucomatous eyes, retardation is lost adjacent to the thicker blood vessels, especially superotemporal and inferotemporal to the optic disc. The deviation maps show areas of flagged pixels (with $P < .5\%$ and $P < 1\%$) superotemporal and inferotemporal to the optic disc. The TSNIT plots are often below the normal range in the temporal part of the superior and inferior bundles in mild-to-moderate glaucoma. In addition, the TSNIT plots in the superotemporal and inferotemporal regions are asymmetrical between eyes. Asymmetries in the nasal sectors are less specific, because they occur in healthy subjects as well. For eyes with severe glaucomatous damage, the TSNIT plot may be flat. The NFI is usually 35 or higher, but some localized defects may not be picked up by this parameter.

DETECTION OF PROGRESSION

Software has recently been introduced to help detect significant RNFL changes compatible with a progressive loss of tissue. Called Guided Progression Analysis (GPA), it is analogous to the tool developed for the analysis of visual field progression. This statistical tool compares the interexamination variability of the individual patient to that observed in a matched population. Reproducible changes in the RNFL can be identified suggestive of glaucomatous progression.

CONCLUSION

SLP has proven to be a useful clinical tool for the assessment and follow-up of eyes with glaucoma and other optic neuropathies. Detecting RNFL loss prior to visual field loss can help the clinican decide to institute therapy earlier, whereas establishing the absence of loss in an eye suspected of being glaucomatous can prevent unnecessary treatment.

Neil T. Choplin, MD, is a glaucoma specialist with Eye Care of San Diego in California. He acknowledged no financial interest in the products or company mentioned herein. Dr. Choplin may be reached at ntchoplin@aol.com.

1. Zhou Q, Knighton RW. Light scattering and form birefringence of parallel cylindrical arrays that represent cellular organelles of the retinal nerve fiber layer. *Appl Opt.* 1997;36:2273-2285.
2. Weinreb RN, Dreher AW, Coleman A, et al. Histopathologic validation of Fourier-ellipsometry measurements of retinal nerve fiber layer thickness. *Arch Ophthalmol.* 1990;108:557-560.
3. Zhou Q, Weinreb RN. Individualized compensation of anterior segment birefringence during scanning laser polarimetry. *Invest Ophthalmol Vis Sci.* 2002;43:2221-2228.
4. Reus NJ, Colen TP, Lemij HG. Visualization of localized retinal nerve fiber layer defects with the GDx with individualized and with fixed compensation of anterior segment birefringence. *Ophthalmology.* 2003;110:1512-1516.
5. Reus NJ, Lemij HG. Diagnostic accuracy of the GDx VCC for glaucoma. *Ophthalmology.* 2004;111:1860-1865.

Confocal Scanning Laser Tomography

By Paul H. Artes, PhD

One of the most rewarding things about my involvement in glaucoma research during the past few years has been to witness the huge changes brought about by technological advances in ocular imaging. The Heidelberg Retina Tomograph (HRT; Heidelberg Engineering GmbH, Heidelberg, Germany) was among the first of such devices, and it is now one of the most useful and reliable workhorses in ophthalmic practice. The instrument is in its third generation, and the company's commitment to the platform's stability has ensured that the data are largely backwards compatible. This means that many centers now have long data series from individual patients with glaucoma, which, in turn, helps to establish and refine techniques for looking at change.

This article reviews some of the practical issues of using the HRT to document the status of the optic nerve head (ONH) and the retinal nerve fiber layer (RNFL) in glaucoma as well as to look for progression.

DIAGNOSIS

The HRT3 provides two analyses to help interpret a single image for the likelihood of damage to the optic disc. The classic approach, the Moorfields Regression Analysis (MRA), compares the neuroretinal rim area of the whole disc, and in

six sectors, to the size of the ONH.[1] The process requires the user to place a contour line along the edge of the optic disc, a fairly easy task that can usually be done within seconds by marking just four points along the cardinal positions.

Another tab in the Eye Explorer software reveals the glaucoma probability score (GPS), a shape analysis of the ONH that does not require a contour line.[2] This option is helpful mostly to inexperienced users who may not yet feel confident about outlining the disc. In most cases, the diagnostic performance of the GPS is similar to that of the MRA.[3] Stereometric parameters derived from the contour line, however, provide quantitative information on the optic disc's size and neuroretinal rim area that can later be used as a comparison with subsequent images.

Both the MRA and GPS tend to "overcall" abnormality in large healthy discs. Caution is also needed with very small ONHs in which a loss of rim area does not become obvious until late in the disease.[3,4] A "quantile regression" approach for the MRA that improves the specificity in large discs was recently published and will, I hope, soon be incorporated into the commercial software.[5]

The HRT does not directly measure the thickness of the RNFL but derives its height profile around the contour line. The familiar double-hump pattern can be a valuable diagnostic sign. One subjective technique that I find particularly useful is to pay attention to the fine striations of the RNFL around the ONH. Owing to the excellent optics and the confocal nature of the scanning system, localized defects in the RNFL often appear much more obvious in the HRT reflectance image than on clinical examination. The "movie" feature of the software provides a slow-motion view along the depth axis through the confocal optical sections, and this can also give a superb view of wedge-type RNFL defects.

PROGRESSION

In a glaucoma practice, perhaps the greatest utility of the HRT lies in its ability to help the clinician assess changes in the optic disc over time. In principle, there are two different approaches for this function. The first is an event-type analysis, which focuses on the difference between the current image and an earlier baseline. The second is a trend-type approach, which derives the rate of change over time in one of the stereometric indices such as rim area. In clinical practice, event-type analyses are arguably more relevant, because physicians must make decisions after short intervals. Trend analyses tend to be more useful with long follow-up (at least 4 years with imaging every 6 months).

The topographical change analysis is an event-type analysis that is a part of the Eye Explorer software of the HRT. This analysis compares the surface height measurements of follow-up images to those of the baseline image. Changes

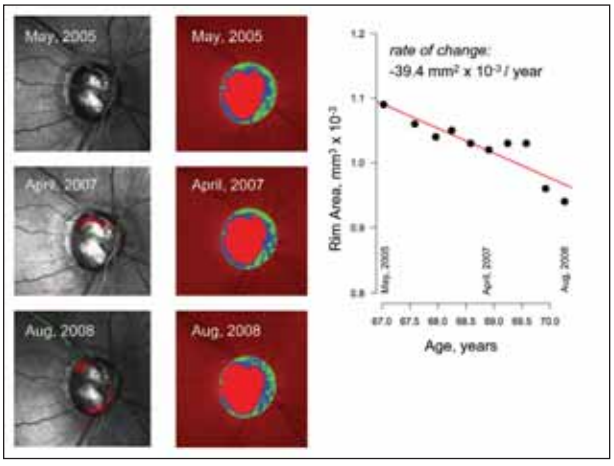

Figure 1. Change in the topography of the optic nerve over a 3-year period in a patient with glaucoma. The topographical change analysis (left) indicates depression at the superior and inferior poles. A loss of rim area (center) is also visible but is most clearly apparent in the plot (right). This indicates a gradual change at a rate of approximately -0.04 mm^{-2}/y.

that are consistent (ie, those that are present in three out of four follow-up images) are highlighted in a color-coded overlay on top of the reflectance image. By inspecting these maps alongside the reflectance and topographic images, clinicians can determine whether and where a change is likely to have taken place (Figure 1).

Of the many stereometric parameters, rim area appears to be the intuitive choice for measuring the speed of change over time. Because the contour line drawn in the baseline image is automatically aligned to the follow-up examinations, an objective rate of change can be derived from a series of measurements over time (Figure 1). Data series with substantial follow-up are now available from several centers, and it is likely that an evidence-based and validated clinical tool for estimating rates of change will be made available within Heidelberg's Eye Explorer software in the near future.

A FEW POINTERS

It is often a good idea to obtain two or even three images during a single session. Once the patient is set up in front of the instrument, the additional imaging only adds a few seconds to the procedure. The quality of the baseline image is critical for subsequent analyses of progression, so selecting the best of several images can greatly increase the odds of detecting subtle change. Also, any variability observed between the images obtained on the first sitting will give the clinician a useful picture of what variation can be expected subsequently, and this will help him or her to interpret any data obtained in the future.

Measuring progression in clinical data is complex. Often, physicians need an answer, even if only approximate, after just a few examinations. This is quite unlike the orthodox approach of testing statistical hypotheses and much more in the spirit of exploratory analysis. A strength of the Eye Explorer software is that it empowers the user in this regard: it is easy to change a baseline examination or to exclude an image of low quality with just a single click of the mouse. By using the software interactively, the clinician can get a much more comprehensive idea of the evidence—something that is impossible to do with a single static printout.

Excellent image quality is critical for the analysis of progression, and images with standard deviations greater than 30 µm are unlikely to be useful for tracking change over time. Moreover, as with other tests, a single "bad apple" can dramatically influence the findings in a series. Clinicians should review both the reflectance and the topographic images, even though it may take a little practice to get familiar with interpreting the false-color representation of the topography.

CONCLUSION

At present, the HRT is the most thoroughly validated tool for assessing structural progression at the optic disc.[6-9] Tools such as the topographical change analysis can help users to gauge change, but they augment and assist rather than replace clinical judgment. Newer technologies such as spectral-domain optical coherence tomography have the potential to provide more precise measurements, but it will take time before the knowledge base and clinical evidence for interpretation reaches the maturity of that available for the HRT. ❑

Paul H. Artes, PhD, is an associate professor and foundation scholar in glaucoma research at Dalhousie University in Halifax, Nova Scotia, Canada. He has received research support from Heidelberg Engineering GmbH and from Optovue Inc. Dr. Artes may be reached at paul@dal.ca.

1. Wollstein G, Garway-Heath DF, Hitchings RA. Identification of early glaucoma cases with the scanning laser ophthalmoscope. *Ophthalmology.* 1998;105:1557-1563.
2. Swindale NV, Stjepanovic G, Chin A, Mikelberg FS. Automated analysis of normal and glaucomatous optic nerve head topography images. *Invest Ophthalmol Vis Sci.* 2000;41:1730-1742.
3. Coops A, Henson DB, Kwartz AJ, Artes PH. Automated analysis of Heidelberg Retina Tomograph optic disc images by glaucoma probability score. *Invest Ophthalmol Vis Sci.* 2006;47:5348-5355.
4. Mardin CY, Horn FK. Influence of optic disc size on the sensitivity of the Heidelberg Retina Tomograph. *Graefes Arch Clin Exp Ophthalmol.* 1998;236:641-645.
5. Artes PH, Crabb DP. Estimating normative limits of Heidelberg Retina Tomography optic disc rim area with Quantile Regression. *Invest Ophthalmol Vis Sci.* 2010;51(1):355-361.
6. O'Leary N, Crabb DP, Mansberger SL, et al. Glaucomatous progression in series of stereoscopic photographs and Heidelberg Retina Tomograph images. *Arch Ophthalmol.* 2010;128(5):560-568.
7. Vizzeri G, Bowd C, Weinreb RB, et al. Determinants of agreement between the confocal scanning laser tomograph and standardized assessment of glaucomatous progression [published online ahead of print June 15, 2010]. *Ophthalmology.* PMID:20557941.
8. Chauhan BC, Hutchison DM, Artes PH, et al. Incidence and rates of visual field progression after longitudinally measured optic disc change in glaucoma. *Ophthalmology.* 2009,116(11):2110-2118.
9. Chauhan BC, Hutchison DM, Artes PH, et al. Optic disc progression in glaucoma: comparison of confocal scanning laser tomography to optic disc photographs in a prospective study. *Invest Ophthalmol Vis Sci.* 2009;50(4):1682-1691.